Hindawi
Mathematical Problems in Engineering
Volume 2021, Article ID 6659598, 15 pages
https://doi.org/10.1155/2021/6659598

Research Article

Vibration Suppression for Beam-Like Repeating Lattice Structure Based on Equivalent Model by a Nonlinear Energy Sink

Gen Liu,[1] **Gongfa Chen**,[1] **and Fangsen Cui**[2]

[1]*School of Civil and Transportation Engineering, Guangdong University of Technology, Guangzhou 510006, China*
[2]*Institute of High Performance Computing, A∗STAR, Singapore*

Correspondence should be addressed to Gongfa Chen; gongfa.chen@gdut.edu.cn

Received 30 October 2020; Revised 12 January 2021; Accepted 19 January 2021; Published 8 February 2021

Academic Editor: Michele Perrella

Based on the fully deployed space beam-like truss, the vibration reduction of the lattice structure is studied by using the local NES (nonlinear energy sink) attachment in this paper. The beam-like lattice structure is modeled as an equivalent linear continuous system (a finite length beam) by the equivalent method and validated with the finite element results. The dynamic vibration equations for the equivalent cantilever beam are established and the governing equations for the equivalent beam with NES are approximated by the Galerkin method. The displacement responses of the beam with and without NES attached under shock excitation are obtained. With NES at different positions, the amplitude responses of the coupled system under the external excitation at different positions are calculated to evaluate the suppression effect of the NES attachment to the structure. And with different masses of the NES, the amplitude responses of the coupled structure subject to the external excitation at different positions are also investigated to get the influence of the mass of the NES attachment to the vibration reduction. It can be seen from the results that the NES attachment can attenuate the response of the beam-like truss under transient excitation efficiently. And with the mass of NES attachment increasing, the vibration amplitude of the coupled system declines more rapidly, and the energy consumption efficiency of the NES attachment is higher. Moreover, the attenuation effect of the NES with different masses is experimentally analyzed. The experimental results are in good accord with the theoretical calculation.

1. Introduction

The deployable structures are mobile assemblies with high strength and high stiffness. Large deployable lattice structures [1] were widely used in space technologies. The solar panels, antennas, radars, and masts of the satellites can be stored in a compact, folded configuration at the launch and were easily deployed into the load-bearing and open forms when working in orbit [2]. This kind of beam-like structure is typically used to deploy solar arrays and scientific instruments and easy to produce complex, multimode, and low-frequency vibrations [3]. Therefore, vibration suppression of the mast is a key problem to be solved in the working condition. Nonlinear energy sink (NES) is an efficient type of strong nonlinear vibration absorber, which has extremely high vibration energy absorption capacity because of its pure nonlinear stiffness. Moreover, due to the small added mass and broadband vibration suppression, the NES is more suitable for vibration reduction than other vibration absorbers in the field of space technologies.

The truss structure is composed of many members and the structure has many degrees of freedom. During the vibration reduction research, so many degrees of freedom will bring difficulties to the dynamic analysis. Timoshenko and Gere [4] studied the approximating method of a lattice truss. The equivalent continuum model could not only simplify the lattice structure but also ensure the accuracy of the research. In the past decades, many researchers focused on the continuum model of lattice structures composed of planar or spatial repeating elements. Nayfeh and Hefzy [5, 6] introduced a construction procedure in order to derive a continuous equivalent model of discrete pin-jointed three-dimensional truss-like periodic structures. Sun and Kim [7] investigated the equivalent stiffness for an extended

Timoshenko beam used to represent the truss beams. For further study, Noor et al. [8] investigated the continuum model for repetitive lattice structures from pin-jointed to rigid-jointed more comprehensively. The effects of the sparse of the truss on the accuracy has been investigated in this paper and the periodic structure approach and substitute continuum approach for continuum models were introduced, which considered local effects in the repeating element. It was found that more repeating elements could not guarantee convergence of the frequency analysis. A classical thin plate continuum model of the large plate-like lattice structure was investigated by Usik [9], and a new energy equivalence technique was proposed. Tollenaere and Caillerie [10] improved the homogenization method and presented continuous modeling of quasirepetitive lattice structures. Burgardt and Cartraud [11] introduced the equivalent beam model into the study of the lattice structure. Odegard et al. [12] established a bridge linking computational chemistry and solid mechanics model through the equivalent continuous model based on the research background of the graphene sheet. In order to analyze the effective stiffness of the three-dimensional stretching control lattice material, Hualin and Wei [13] used the equivalent continuum method. Using the homogenization method, Salehian and Inman [14] presented a dynamic analysis of the truss structures for large satellite applications. A simple small order micropolar continuum model for a planer truss structures with flexible joints was introduced. A spatial equivalent continuum model for the planar rigid-jointed repeating element was established by Liu et al. [15]; then an equivalent circular ring model was presented for the ring truss. The linear truss was a spatial structure. From the perspective of simplification, this paper focuses on studying the vibration reduction of the plane truss and then further investigating the vibration reduction of space truss structure with the equivalent methods. Moreover, nanobeams and microbeams [16–19] also can be modeled via lattice equivalent to investigate its bending response.

The study of the targeted energy transfer (TET) dynamics to the linear discrete system and linear elastic continua system attached NES began more than ten years ago. The realization of TET was firstly observed by Gendelman [20] who studied the transient dynamics of a two-DOF system consisting of a damped linear oscillator that was weakly coupled to an essentially nonlinear, damped attachment. In the initial study, the essentially nonlinear oscillators attached to different linear discrete structures could act as broadband passive absorbers of the vibration energy. The responses of linear structures coupled to essential nonlinearity attachment were complex. Meanwhile, one-way vibration suppression from the main structure to a local essentially nonlinear attachment occurred [21, 22]. Moreover, different configurations of the attachment and more degrees of freedom of the system were studied by many researchers [23, 24]. Some experimental evidence of nonlinear energy pumping was obtained in the research [25] at the same time. In contrast to the classical linear vibration absorber, the NES may passively absorb broadband energy over wide frequency ranges.

While many achievements have been made in the study of discrete systems attached NES [26], the passive targeted energy transfer [27–31] was extended to the continuum system. Georgiades and Vakakwas provided numerical evidence of passive targeted energy transfer from a linear flexible beam under shock excitation to a local essentially nonlinear lightweight attachment [32, 33]. The first class of linear elastic systems which were composed of linear rods or beams with attached NESs were investigated by Georgiades and Vakakis [34], Tsakirtzwas et al. [35], and Panagopoulos et al. [36]. Vakakwas [37] summarized the subject of passive vibration control of mechanical systems subjected to broadband, transient inputs by summarizing from a series of papers and presentations. Targeted energy transfer (TET) was introduced, which represented a new and unique approach to the passive control problem.

Up to now, research on vibration reduction of linear systems of coupled oscillators to attached NESs was paid attention to. Ahmadabadi and Khadem [38] investigated the effect of an attached nonlinear energy sink on energy suppression of a cantilever beam under shock excitation. Vibration suppression of an axially moving beam with NESs under shock-induced vibration by Zhang et al. [39]. Kani et al. [40] investigated targeted energy transfer from a nonlinear continuous system to a nonlinear energy sink (NES) using the new method to obtain the optimized parameters of the NES. Fang et al. [41] focused on the transient nonlinear dynamics and targeted energy transfer (TET) of a Bernoulli–Euler beam coupled to a continuous bistable nonlinear energy sink (NES). The performance of a smooth nonlinear energy sink (NES) to mitigate vibration of a rotating Euler–Bernoulli beam under an external force was investigated by Bab et al. [42]. Kremer and Liu [43, 44] investigated energy harvesting using a nonlinear energy sink. The research achieved simultaneous vibration suppression and energy harvesting using a variant form of nonlinear energy sink (NES). Chen et al. [45] analyzed the effects of nonlinear energy sink (NES) on vibration suppression of a simply supported beam and it was found that parallel NES can eliminate the higher branches of the system more effectively by tuning nonlinear stiffness and damping. Moreover, the effects of nonlinear energy sink on vibration reduction of a truss core sandwich beam under the impulse and harmonic loads [46] were studied. The results showed that the vibration suppression was enhanced by increasing the damping of NES when the system was excited by harmonic load and with decreasing the damping when the system was excited by impulse loads.

Although previous researchers have done a lot of work on vibration reduction of the linear system through targeted energy transfer method, they rarely focused on the vibration suppression of lattice structure attached NESs. And local attachment-NESs based on the beam equivalent from the truss structure can be used in the nanobeams and microbeams to solve vibration suppression of the structure. The novelty of this paper was that the vibration suppression of the lattice structure was studied by using the local attachment-NESs based on the beam equivalent from the truss structure. The organization of the paper is that the model of the beam-

like lattice structure was built as an equivalent linear continuous system firstly; then, the vibration reduction effects of the absorber on the cantilever beam under shock loads and the influence of the mass of the NES attachment to the attenuation efficiency were investigated. Lastly, to verify the methods proposed in this paper, an experimental analysis of the beam attached NES was carried out to validate the theoretical calculation.

2. Equivalent Beam Model

The X-brace girder structure consists of repeated cells in the axis direction. The planar beam-like lattice structures (X-brace girder) attached NES are shown in Figure 1.

For the purpose of establishing a continuum model, an equivalent beam is defined to have the same amount of the strain energy and the kinetic energy stored in it as those of the original lattice grid when both are deformed identically in Figure 2. Firstly, the repeating element is isolated from the grid, and the strain energy and the kinetic energy are derived in terms of the nodal displacements, velocities, and material properties of each lattice member.

The displacements components of any cross section in the plane [36] are as follows:

$$u = u^0 + y\varphi^0 = u^0 + y\left.\frac{\partial u}{\partial y}\right|_{y=0}, \tag{1a}$$

$$v = v^0 + y\varepsilon_y^0 = v^0 + y\left.\frac{\partial v}{\partial y}\right|_{y=0}, \tag{1b}$$

displacements at $y = 0$ and ε_y^0 is the extensional strain in the y direction.

The displacement components u^i, v^i at a typical node i of the repeating element are expanded in the Taylor series in terms of the original displacement components, u_0 and v_0. The expressions of the displacements can be written in the following form:

$$u = u^0 + y^i\varphi^0 + x^i\left(\varepsilon_x^0 + y^i\kappa_x^0\right) + \frac{1}{2}\left(x^i\right)^2\left(\frac{\mathrm{d}\varepsilon_x^0}{\mathrm{d}x} + y^i\frac{\mathrm{d}\kappa_x^0}{\mathrm{d}x}\right), \tag{2a}$$

$$v = v^0 + y^i\varepsilon_y^0 + x^i\left[\frac{\mathrm{d}v^0}{\mathrm{d}x} + y^i\frac{\mathrm{d}\varepsilon_y^0}{\mathrm{d}x}\right] + \frac{1}{2}\left(x^i\right)^2\left[\left(\frac{\mathrm{d}\gamma_{xy}^0}{\mathrm{d}x} - \kappa_x^0\right) + y^i\frac{\mathrm{d}^2\varepsilon_y^0}{\mathrm{d}x^2}\right], \tag{2b}$$

where $\varepsilon_x^0 = (\mathrm{d}u^0/\mathrm{d}x)$, $\varphi^0 = (\mathrm{d}v^0/\mathrm{d}x) - \gamma_{xy}^0$, and $\kappa_x^0 = (\mathrm{d}\varphi^0/\mathrm{d}x)$.

By Taylor expansions of the displacement variables, the strains are obtained: the extensional strains ε_x^0 in the x directions, ε_y^0 in the y direction, the shearing strain γ_{xy}^0, and the curvature κ_x^0.

The expression of the strains energy for the lattice structure is given by

$$U = \frac{1}{2}L\varepsilon^t C\varepsilon, \tag{3}$$

where $\varepsilon^t = \begin{bmatrix}\varepsilon_x^0 & \kappa_x^0 & \gamma_{xy}^0\end{bmatrix}$.

Therefore, equation (3) can be rewritten as

$$U = \sum\frac{1}{2}\Delta_1^t\Gamma^{(m)t}K^{(m)}\Gamma^{(m)}\Delta_1, \tag{4}$$

where $\Delta_1^t = \begin{bmatrix}u^i & v^j & u^j & v^j\end{bmatrix}$. The term $K^{(m)}$ is the stiffness matrix in the local coordinates and $\Gamma^{(m)}$ is the transformation matrix from the local coordinates of a typical member m to the coordinates of the repeating element.

The expressions of the kinetic energy for the repeating element is given by

$$T = \frac{1}{2}L\rho_0\left[\left(\frac{\partial u^0}{\partial t}\right)^2 + \left(\frac{\partial v^0}{\partial t}\right)^2\right] + \frac{1}{2}L\rho_1\left(\frac{\partial\varphi^0}{\partial t}\right)^2. \tag{5}$$

Substituting equations (2a) and (2b) into (5), the kinetic energy can be expressed as

$$T = \frac{1}{2}\sum\Delta_2^t\Gamma^{(m)t}M^{(m)}\Gamma^{(m)}\Delta_2, \tag{6}$$

where $\Delta_2^t = \begin{bmatrix}(\partial u^i/\partial t) & (\partial v^j/\partial t) & (\partial u^j/\partial t) & (\partial v^j/\partial t)\end{bmatrix}$.

Based on Hamilton's principle and the energy equivalence method [14], the mechanical parameters C of the equivalent continuum model can be determined by the same strain energy and kinetic energy of the periodic truss unit and the equivalent continuum model in the same deformation mode. The governing ordinary differential equations of the beam for the lattice structure can be written in the following form:

$$C_{11}\frac{\partial^2 u^0}{\partial x^2} + C_{13}\frac{\partial^2 v^0}{\partial x^2} + C_{12}\frac{\partial^2\varphi^0}{\partial x^2} + C_{13}\frac{\partial\varphi^0}{\partial x} = \rho_0\frac{\partial^2 u^0}{\partial t^2}, \tag{7a}$$

$$C_{13}\frac{\partial^2 u^0}{\partial x^2} + C_{33}\frac{\partial^2 v^0}{\partial x^2} + C_{33}\frac{\partial\varphi^0}{\partial x} = \rho_0\frac{\partial^2 v^0}{\partial t^2}, \tag{7b}$$

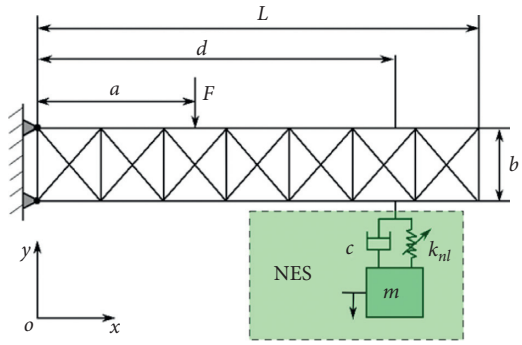

Figure 1: The truss structure with additional NES attachment.

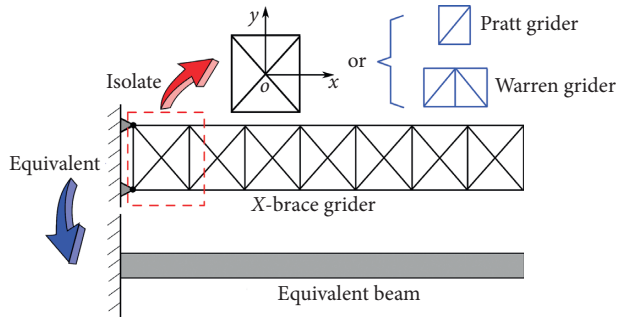

Figure 2: The equivalent beam model of the plane truss.

$$C_{12}\frac{\partial^2 u^0}{\partial x^2}+(-C_{13})\frac{\partial u^0}{\partial x}+(-C_{33})\frac{\partial v^0}{\partial x}+C_{22}\frac{\partial^2 \varphi^0}{\partial x^2}+(-C_{33})\varphi^0=\rho_1\frac{\partial^2 \varphi^0}{\partial t^2}, \tag{7c}$$

where the parameter C_{11} is the extensional stiffness of the beam; C_{22} is the bending stiffness of the beam; C_{33} is the shear stiffness; C_{12} and C_{13} are the stiffness coupling coefficients.

Figure 3 gives three classical lattice models. For different lattice structures, there will be different coefficients C for the equivalent beam structure. The X-brace structure is considered here based on equations (7a)–(7c), and the governing differential equations and coefficients of the equivalent beams are as follows:

$$C_{11}\frac{\partial^2 u^0}{\partial x^2}=\rho_0\frac{\partial^2 u^0}{\partial t^2}, \tag{8a}$$

$$C_{33}\frac{\partial^2 v^0}{\partial x^2}+C_{33}\frac{\partial \varphi^0}{\partial x}=\rho_0\frac{\partial^2 v^0}{\partial t^2}, \tag{8b}$$

$$(-C_{33})\frac{\partial v^0}{\partial x}+C_{22}\frac{\partial^2 \varphi^0}{\partial x^2}+(-C_{33})\varphi^0=\rho_1\frac{\partial^2 \varphi^0}{\partial t^2}, \tag{8c}$$

where

$$\begin{aligned}
C_{11}&=\frac{\left(48L_lI_dL_vA_dE_d^2\left(L_l^2+L_v^2\right)^2\right.}{\left(2A_dL_d^5L_v^3+24I_dL_l^2L_l^3L_v\right)E_d+L_d^8A_vE_v}+\frac{2L_d^5E_dA_d\left(2A_lE_lL_v^3+A_vE_vL_l^3\right)}{\left(2A_dL_d^5L_v^3+24I_dL_l^2L_l^3L_v\right)E_d+L_d^8A_vE_v}\\
&\quad+\frac{48L_d^3E_d\left(I_dL_vL_l\left(L_lA_lE_l+(1/2)L_vA_vE_v\right)\right)}{\left(2A_dL_d^5L_v^3+24I_dL_l^2L_l^3L_v\right)E_d+L_d^8A_vE_v}+\frac{2A_lA_2E_lE_vL_d^8}{\left(2A_dL_d^5L_v^3+24I_dL_l^2L_l^3L_v\right)E_d+L_d^8A_vE_v},\\
C_{22}&=\frac{1}{2L_v}\left(L_lE_lL_v^3+6E_vI_vL_l\right),\\
C_{33}&=\frac{6E_dI_dL_l^5L_v-12E_dL_v^3L_l^3\left(I_d-(1/6)A_dL_v^2\right)}{L_l^2L_vL_d^5}+\frac{L_l\left(3E_vI_vL_v^5+6E_dI_dL_v^5\right)}{L_l^2L_vL_d^5}.
\end{aligned} \tag{9}$$

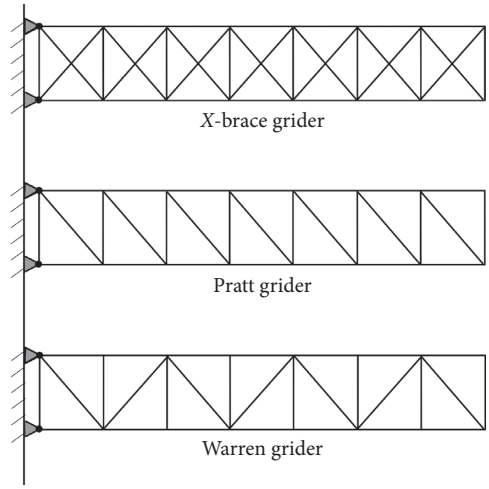

Figure 3: Configurations of the three classical plane truss.

For the slender cantilever space structure, the Euler–Bernoulli beam theory can be applied to the truss structure, and the low order bending vibrations are worth considering. Therefore, ignoring the effect of the angle φ, the dynamic equation of the transverse vibration of the structure is obtained:

$$C_{33}\frac{\partial^4 v(x,t)}{\partial x^4} + m_0\frac{\partial^2 v(x,t)}{\partial t^2} = f(x,t), \tag{10}$$

where C_{33} is the equivalent bending stiffness; m_0 is the equivalent mass coefficient; and $f(x,t)$ is the uniform loads imposed on the beam.

To test and evaluate the accuracy of the predictions of the equivalent beam model, the natural frequency of the equivalent model is compared with that of the truss structure. The first two-order modes of the cantilever beam are considered. For the X-brace lattice with ten bays, the lowest two vibration modes and frequencies obtained by the equivalent beam are shown in Figure 4.

Figure 5 depicts the relative values of the frequencies between the equivalent model and FEM model. It is observed from Figure 5 that the largest error is 8% in the second-order bending modes and the smallest error is 4% in the first-order bending modes and the errors are within the acceptable range. It can be said that, for the slender lattice structure, the equivalent modeling using the Euler–Bernoulli beam theory can reflect the vibration characteristics of the original structure better.

3. Dynamical Model and Transient Response Analysis

Considering that the beam-like lattice structure is slender, the dynamic vibration equations of the beam coupled with NES are built by the linear Bernoulli–Euler theory:

$$C_{33}\frac{\partial^4 v(x,t)}{\partial x^4} + m_0\frac{\partial^2 v(x,t)}{\partial t^2} + \varepsilon\lambda\frac{\partial v(x,t)}{\partial t} + \left\{k_{nl}[v(d,t) - w(t)]^3 + \varepsilon\lambda\left[\frac{\partial v(d,t)}{\partial t} - \dot{w}(t)\right]\right\}\delta(x-d) = f(t)\delta(x-a), \tag{11a}$$

$$\varepsilon m_0\ddot{w}(t) + k_{nl}[w(t) - v(d,t)]^3 + \varepsilon\lambda\left[\dot{w}(t) - \frac{\partial v(x,t)}{\partial t}\right] = 0, \tag{11b}$$

where $(\bullet)_{xxxx}$ donates $(\partial^4(\bullet)/\partial x^4)$ and $(\bullet)_t$ donates $\partial(\bullet)/\partial t$. $C_{33}$is the bending stiffness of the equivalent beam and m_0 represents the mass per unit length of the beam. λ is the damping of the NES and k_{nl} is the nonlinear stiffness parameter of the attachment and the term before k_{nl} is the cubic nonlinear stiffness. There is an assumption that the NES is lightweight compared to the mass of the beam, which is important for the engineering applications, especially in the field of aerospace technology. It is supposed the mass of the NES attachment is ε that of the spacecraft structure, and the range of the parameter ε is $0 < \varepsilon \ll 1$.

Due to the lightweight of the NES attachment, the cantilever beam structure modal function [47] is used when selecting the equivalent beam structure modal:

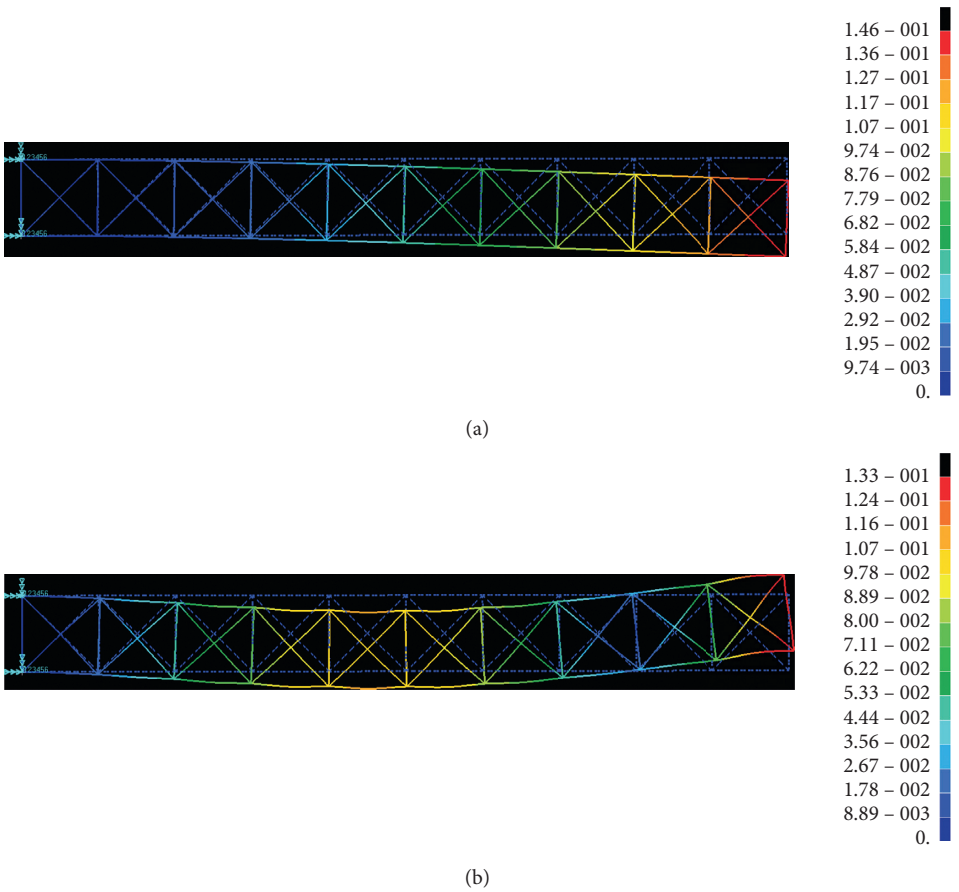

Figure 4: The first two-order modes of the equivalent model. (a) The first-order mode. (b) The second-order mode.

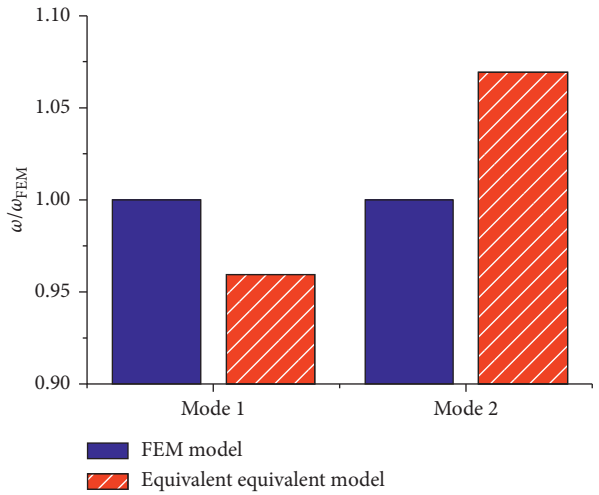

Figure 5: The relative values of the frequencies between the equivalent model and FEM model.

$$\varphi_i(x) = \cos\beta_i x - ch\beta_i x + \xi_i\left(\sin\beta_i x - sh\beta_i x\right), \quad (i = 1, 2, \ldots),$$
$$\omega_i = \left[\frac{(2i-1)\pi}{2l}\right]^2 \sqrt{\frac{\mathrm{EI}}{\rho S}}, \quad (i = 1, 2, \ldots), \tag{12}$$

where $\xi_i = -\cos\beta_i l + ch\beta_i l/\sin\beta_i l + sh\beta_i l$ and $\beta_i l$ are obtained by solving the equations as follows:

$$\cos\beta_i l\, ch\beta_i l + 1 = 0, \quad (i = 1, 2, 3)$$
$$\beta_i l \approx \left(\frac{2i-1}{2}\right)\pi, \quad (i = 4, \ldots). \tag{13}$$

The damped beam-NES coupled system is non-dimensionalized by introducing the following dimensionless parameters and variables:

$$\tau = t\frac{\mathrm{EI}}{m},$$
$$k_{nl} = \frac{K_{nl}}{\mathrm{EI}},$$
$$\lambda_1 = \frac{\varepsilon\lambda}{m}, \tag{14}$$
$$\varepsilon_1 = \frac{\varepsilon}{m},$$
$$q(x,\tau) = \frac{f(x,\tau)}{m\mathrm{EI}}.$$

Substituting equations (14) into (11a) and (11b), the nondimensional governing equations of the coupled system are given:

$$\frac{\partial^4 v(x,\tau)}{\partial x^4} + \frac{\partial^2 v(x,\tau)}{\partial \tau^2} + \lambda_1\frac{\partial v(x,\tau)}{\partial \tau} + \left\{k_{nl}[v(d,\tau) - w(\tau)]^3 + \lambda_1\left[\frac{\partial v(d,\tau)}{\partial \tau} - \dot{w}(\tau)\right]\right\}\delta(x-d) = q(\tau)\delta(x-a), \tag{15a}$$

$$\varepsilon_1\ddot{w}(\tau) + k_{nl}[w(\tau) - v(d,\tau)]^3 + \lambda_1\left[\dot{w}(\tau) - \frac{\partial v(x,\tau)}{\partial \tau}\right] = 0. \tag{15b}$$

The transverse displacement field can be expressed as

$$v(x,\tau) = \sum_{i=1}^{\infty} a_i(\tau)\varphi_i(x). \tag{16}$$

Substituting equations (17a) and (17b) into (15a) and (15b), the following equations are obtained:

$$\sum_{i=1}^{\infty} a_i(\tau)\frac{\partial^4\varphi_i(x)}{\partial x^4} + \sum_{i=1}^{\infty}\ddot{a}_i(\tau)\varphi_i(x) + \lambda_1\sum_{i=1}^{\infty}\dot{a}_i(\tau)\varphi_i(x) + \left\{k_{nl}\left[\sum_{i=1}^{\infty}a_i(\tau)\varphi_i(d) - w(\tau)\right]^3 + \lambda_1\left[\sum_{i=1}^{\infty}\dot{a}_i(\tau)\varphi_i(d) - \dot{w}(\tau)\right]\right\}\delta(x-d) = q(\tau)\delta(x-a), \tag{17a}$$

$$\varepsilon_1\ddot{w}(\tau) + k_{nl}\left[w(\tau) - \sum_{i=1}^{\infty}a_i(\tau)\varphi_i(d)\right]^3 + \lambda_1\left[\dot{w}(\tau) - \sum_{i=1}^{\infty}\dot{a}_i\varphi_i(d)\right] = 0. \tag{17b}$$

Multiplying equations (17a) and (17b) by $\varphi_i(x)$, integrating them with respect to x from 0 to L, and using the orthogonality principle, the following set of coupled nonlinear ordinary differential equations can be obtained:

$$\ddot{a}(\tau) + \beta\dot{a}(\tau) + \omega^2 a(\tau) + k_{nl}\left[\sum_{i=1}^{\infty} a_i(\tau)\varphi_i(d) - w(\tau)\right]^3 \varphi_p(d) + \lambda_1\left[\sum_{i=1}^{\infty} \dot{a}_i(\tau)\varphi_i(d) - \dot{w}(\tau)\right]\varphi_p(d) = F(\tau)\varphi_p(d), \tag{18a}$$

$$\varepsilon_1\ddot{w}(\tau) + k_{nl}\left[w(\tau) - \sum_{i=1}^{\infty} a_i(\tau)\varphi_i(d)\right]^3 + \lambda_1\left[\dot{w}(\tau) - \sum_{i=1}^{\infty} \dot{a}_i\varphi_i(d)\right] = 0, \tag{18b}$$

where $a(\tau)$ and $w(\tau)$ are, respectively, the displacements of the beam and the NES.

Equations (18a) and (18b) are used to analyze the dynamic characteristics of the equivalent beam coupled system with additional NES. In the field of aerospace applications, external loads tend to be imposed at the free end of the linear trusses. The displacement of the free end should be as small as possible so that it can be in a good working condition. For this beam-like truss structure, its first-order bending mode is considered here, which means $i = 1$ in equations (18a) and (18b). The effects of NES on the attenuation of the end amplitude are investigated.

The position of the external excitation is exerted at two positions, that is, the fixed end and the free end. The position of the NES attachment moves between the fixed end and the free end of the equivalent beam.

The attenuation effects of NES in different positions on the equivalent beam with the external load imposed at the free end are observed. The relevant dimensionless parameters are as follows:

$$\begin{aligned} \beta &= 0.1, \\ \omega &= 10, \\ k_{nl} &= 1000, \\ \lambda &= 0.5, \\ \varepsilon &= 0.1. \end{aligned} \tag{19}$$

Figures 6(a)–6(g) give the displacement responses of the free end of the structure and that of the NES with the external loads been excited at the free end of the equivalent beam and the NES in different positions. It can be seen from Figures 6(a)–6(g) that when the excitation is at the free end, the beam axis deviates from the central position from the free end to the fixed end direction. The response amplitude of NES also varies with the excitation position, and the amplitude of NES response is enlarging when the beam axis deviates from the center position. Figure 6(h) gives the attenuation effect of the transverse displacement of the beam after 10 seconds when the excitation is at the free end and the NES is in different positions.

In Figure 6(h), A_1 is the response amplitude of the beam at the initial stage when the excitation is at the free end, A_2 is the displacement response of the beam after 10 seconds, and A_3 is the attenuation efficiency of the beam response displacement in 10 seconds when the NES is in a different position. It can be seen that even though the initial response displacement of the NES is large, the attenuation efficiency of the beam displacement response is also great. Generally speaking, the contribution of NES to the attenuation of beam displacement response has high efficiency in different positions.

When the excitation force is at the fixed end of the equivalent beam and the NES is located at different positions, Figures 7(a)–7(g) depict the displacement responses of the free end of the structure and that of the NES.

It can be seen from Figures 7(a)–7(g) that when the excitation is at the fixed end of the beam, the position of the beam center deviating from the center line is gradually decreasing along the free end to the fixed end direction. The response amplitude of NES also varies with the excitation position, and the amplitude of NES response is larger when the beam axis deviates from the center position. Figure 7(h) gives the attenuation effect of the transverse displacement of the beam after 10 seconds when the excitation is at the fixed end and the NES is in different positions. In Figure 7(h), B_1 is the response amplitude of the beam at the initial stage when the excitation is at the fixed end, B_2 is the displacement response of the beam after 10 seconds, and B_3 is the attenuation efficiency of the beam response displacement in 10 seconds with the NES in a different position. It can be found that when the initial response displacement of the NES is large, the attenuation efficiency of the beam displacement response is also great. Similarly, when the excitation is at the fixed end of the beam, the NES has a higher attenuation efficiency to the beam's displacement response.

Figure 8 gives a comparison of the attenuation effects of NES on the transient response of a cantilever beam at the free end with different mass ratios. The initial displacement response of the cantilever beam is 0.1, the mass of the NES is large, and the transient response attenuation of the cantilever beam decays rapidly. It can be seen from Figure 8 that, with the increasing of the mass ratio, the time of displacement amplitude response attenuation to 25% of the initial displacement is gradually reduced. As the mass of NES

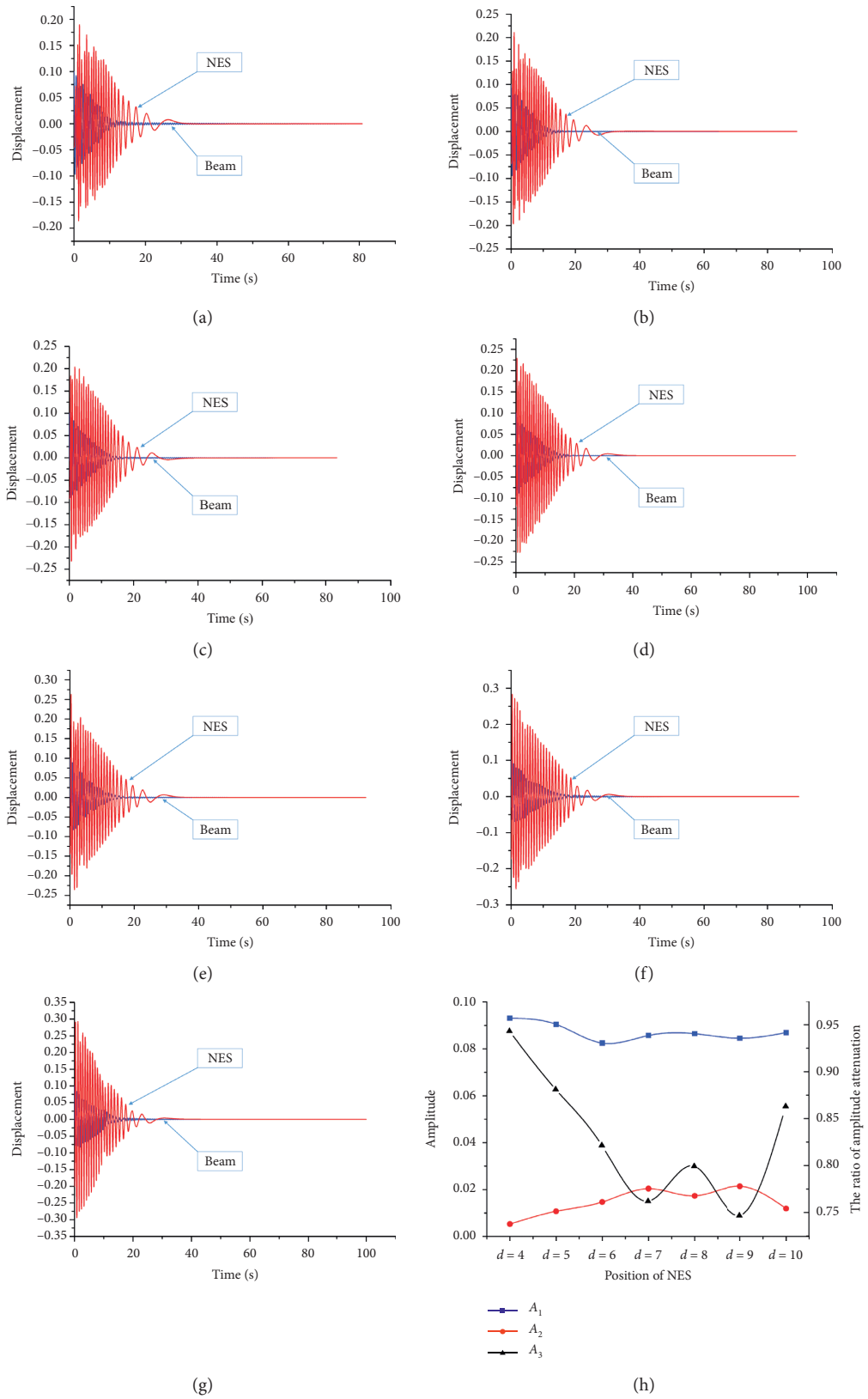

Figure 6: The attenuation effects of NES in different positions on the equivalent beam with the external load imposed at the free end. (a) $d = 4$ m. (b) $d = 5$ m. (c) $d = 6$ m. (d) $d = 7$ m. (e) $d = 8$ m. (f) $d = 9$ m. (g) $d = 10$ m. (h) The ratio of the amplitude attenuation.

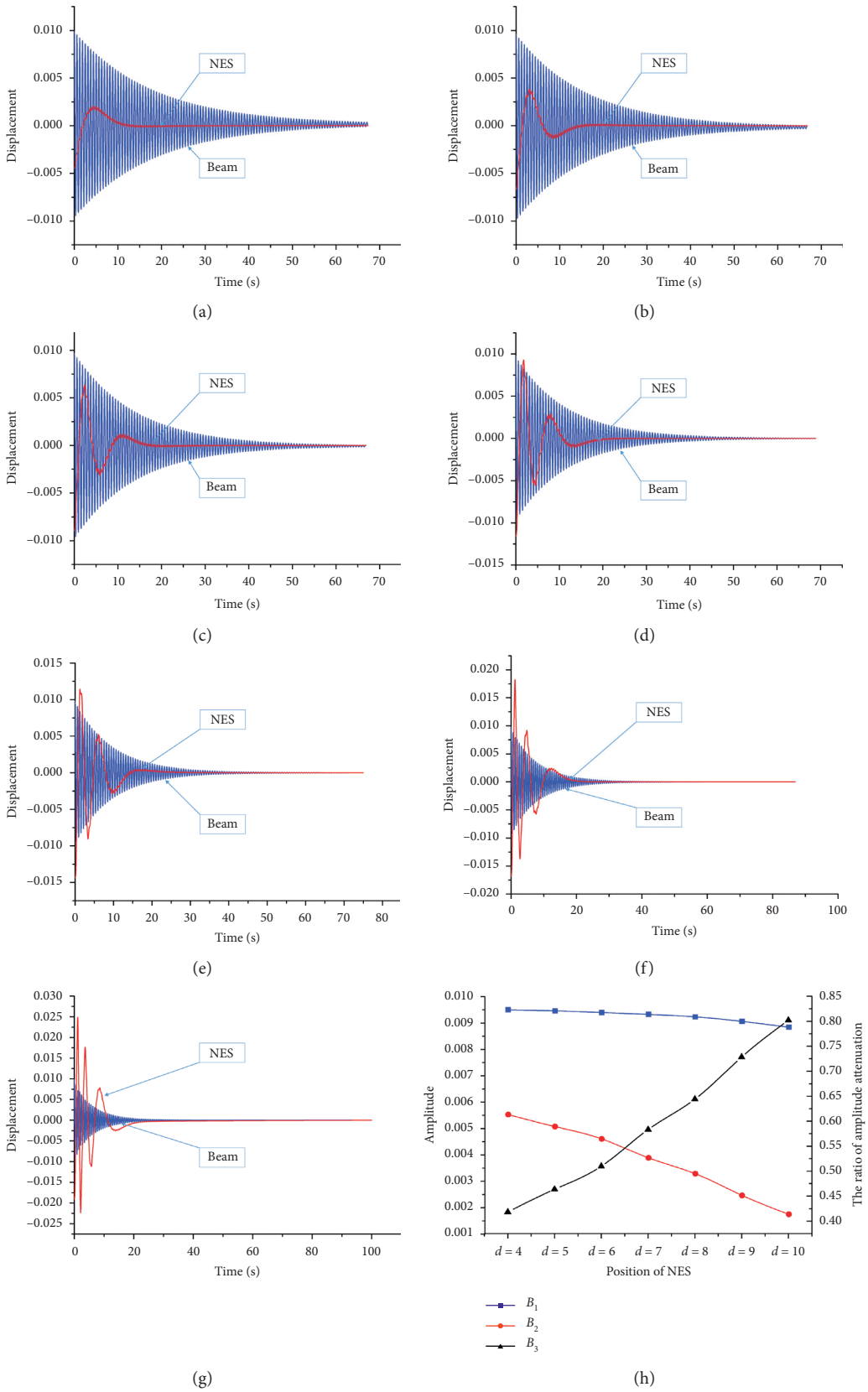

Figure 7: The attenuation effects of NES in different positions on the equivalent beam with the external load imposed at the fixed end. (a) $d = 4$ m. (b) $d = 5$ m. (c) $d = 6$ m. (d) $d = 7$ m. (e) $d = 8$ m. (f) $d = 9$ m. (g) $d = 10$ m. (h) The ratio of the amplitude.

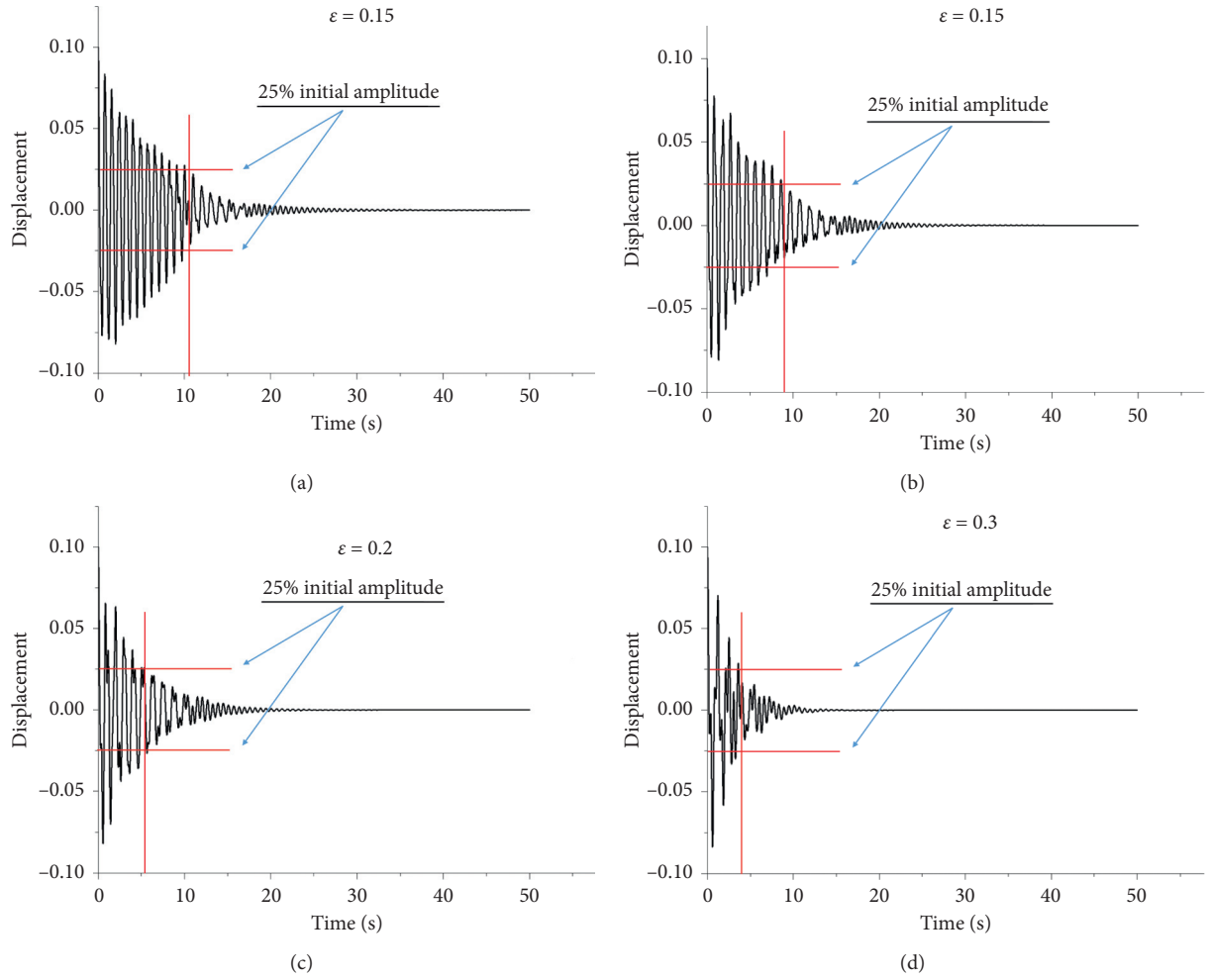

Figure 8: Attenuation effect of NES with different mass ratios. (a) $\varepsilon = 0.1$. (b) $\varepsilon = 0.15$. (c) $\varepsilon = 0.2$. (d) $\varepsilon = 0.3$.

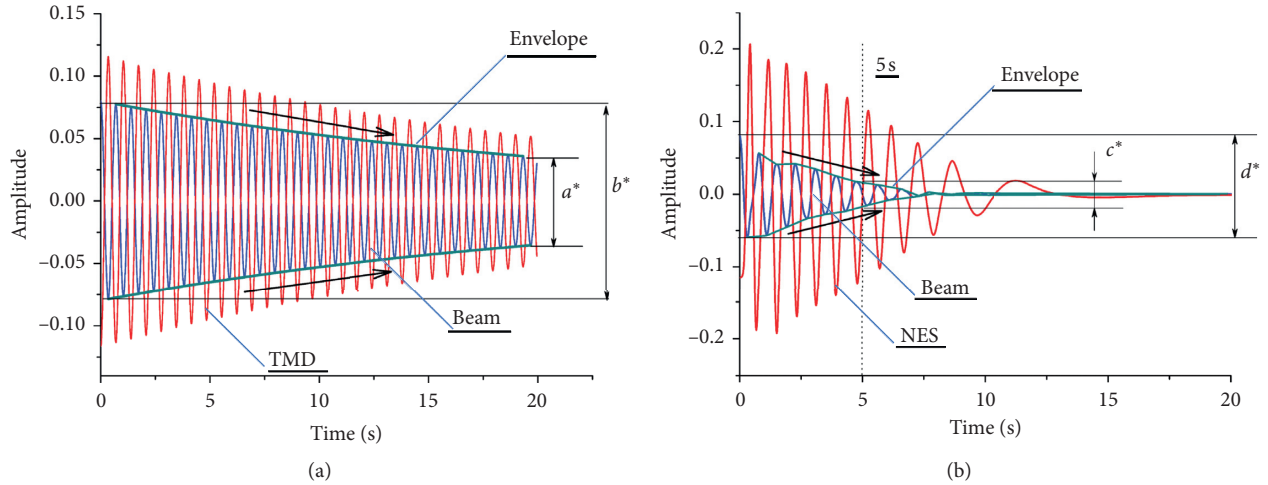

Figure 9: The displacement response attenuation of the coupled system with different vibration absorbers. (a) The additional linear stiffness damping absorber. (b) The additional NES absorber.

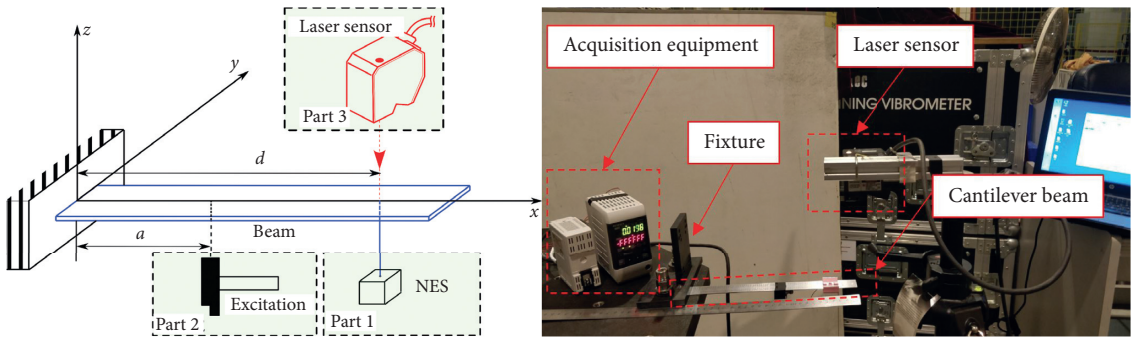

Figure 10: Experimental equipment layout.

Table 1: Physical parameters of the cantilever beam.

Beam	Length (mm)	Width (mm)	Thickness (mm)	Material
	350	27	1	Stainless steel

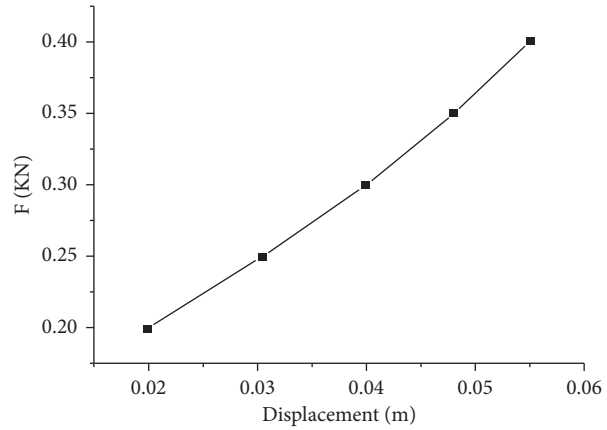

Figure 11: Stiffness curve of the nonlinear spring.

attachment increases, the vibration amplitude of the coupled system declines more rapidly, and the energy consumption efficiency of NES attachment is higher. It can be obtained that the quality of the NES has an important effect on the attenuation effect of the transient response of the cantilever beam.

Compared with the linear stiffness damping damper, the NES passive damping effect has obvious advantages. Figure 9 demonstrates the displacement response attenuation of the coupled system with the case that the excitation has the value 2 and the location of the NES is 9.

Due to the coupling effect of the nonlinear coupled system, although the initial response of the equivalent cantilever structure with additional NES is larger than that of the linear shock absorber coupling structure, the attenuation effect of the additional NES structure is obvious. Comparing the initial attenuation amplitude a^*, b^* of the additional linear stiffness damping structure in Figure 9(a), and the attenuation amplitude c^*, d^* of the additional NES in Figure 9(b), it is can be found that the attenuation of the structure amplitude reaches a considerable degree in 5 seconds with additional NES once the excitation is imposed, and the trend of amplitude decline is even steeper, which can demonstrate the good vibration reduction effect of NES.

4. Frequency Analysis

After analyzing the overall amplitude response of the coupled system, the following experiments are designed to verify some results obtained in the theoretical calculation. Figure 10 presents a schematic diagram of the experimental study of the transient response attenuation of a cantilever beam with additional NES.

In Figure 10, the transient response of transverse displacement of the cantilever beam is investigated. The arrangement of the measuring device is divided into three parts. Part 1 is the NES vibration absorber attachment composed of nonlinear spring and mass, Part 2 is the cantilever beam excitation configuration, and Part 3 is the cantilever beam response displacement acquisition device. The position of the NES attachment is at the axis of the beam. During the test, the position of the NES is moving along the axis x to investigate its vibration amplitude attenuation effect of the coupled system. The excitation is also applied to the

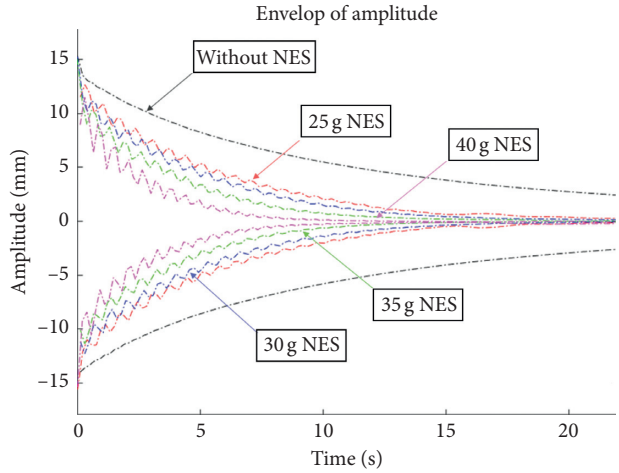

Figure 12: Envelope of the time-domain curve of transient response attenuation of structures with different masses of NES and without NES.

axis of the beam, perpendicular to the plane. The collection point of vibration amplitude is selected on the axis to avoid the amplitude caused by out-of-plane vibration affecting the accuracy of experimental data. The geometrical parameters and the material parameters of the beam are shown in Table 1.

In the test, in order to obtain the nonlinear stiffness parameter of the NES, different elastic rubber ropes are selected for static loading experiments, and the force-displacement curve in Figure 11 is obtained. From the curve trend in Figure 11, it is can be seen that the spring stiffness curve has the characteristic of the cubic nonlinear spring.

Weights of different NES masses are selected as 20 g, 30 g, 35 g, and 40 g, as shown in Figure 12 so as to obtain the attenuation efficiency on the structure with different mass coefficients. The amplitude acquisition device adopts the KEENES laser single point vibration displacement collector, which provides high experimental acquisition accuracy and acquisition rate.

The time-domain curve of the transient response of the transverse displacement of the cantilever beam is obtained with different NES qualities and is used to compare the transient response of transverse displacement of a cantilever beam with different mass ratios in the theoretical calculation. Figure 12 gives the time-domain curve of the transverse displacement response of the cantilever beam with different NES mass and without NES. By applying the same displacement excitation (15 mm) to the free end of the beam, it can be seen that the higher the NES mass is, the greater the efficiency of the transient response attenuation of the beam structure will be. Therefore, the correctness of the theoretical calculation is verified by the experimental results.

5. Conclusions

In this paper, the beam-like lattice structure is modeled as an equivalent linear continuous system by the equivalent method and validated with the finite element results. The dynamic vibration equations for the equivalent cantilever beam are established and the governing equations for the equivalent beam with NES are approximated by the Galerkin method to carry out the numerical calculations. For NES with different masses, an experiment is designed to verify the theoretical results of the transient transverse displacement response of the beam. The experimental results verify the theoretical results well. Some results are gained:

(1) The attenuation effects of NES in different positions on the equivalent beam with the external load imposed at the free end are observed. The results showed that the response amplitude of NES also varies with the excitation position, and the amplitude of NES response is enlarging when the beam axis deviates from the center position.

(2) The attenuation effects of NES in different positions on the equivalent beam with the external load imposed at the fixed end are investigated. It can be found from the numerical results that even though the initial displacement response of the NES is large, the attenuation efficiency of the beam displacement response is also great.

(3) The attenuation effects of NES on the transient response of a cantilever beam at the free end with different mass ratios are investigated. With the increase in the mass ratio, the time of displacement amplitude response attenuation to 25% of the initial displacement is gradually reduced. As the mass of NES attachment increases, the vibration amplitude of the coupled system declines more rapidly, and the energy consumption efficiency of NES attachment is higher. It can be obtained that the quality of the NES has an important effect on the attenuation effect of the transient response of the cantilever beam.

(4) The better vibration reduction effect of NES than the linear stiffness damping absorber is found in this paper. The attenuation of the structure amplitude reaches a considerable degree in 5 seconds with

additional NES once the excitation is imposed, and the trend of amplitude decline is steeper.

The relevant dynamic analysis of the equivalent continuum can not only effectively reflect the dynamic characteristics of the structure but also reduce the computational workload. In future study, new numerical examples such as the toy model to explain all the key steps of the approach can be done to verify the theoretical results proposed in the paper.

Data Availability

No data were used to support this study.

Conflicts of Interest

The authors declare that they have no conflicts of interest.

Acknowledgments

This work was supported by the Key R&D projects of the Ministry of Science and Technology of China (Grant no. 2016YFE0117200).

References

[1] W. Zhang, A. Xi, B. Siriguleng, and G. Liu, "An equivalent cylindrical shell model of vibration analysis based on simplified repeating unit cell for ring truss structure," *Journal of Sound and Vibration*, vol. 459, Article ID 114847, 2019.

[2] C. Gantes, J. J. Connor, and R. D. Logcher, "Equivalent continuum model for deployable flat lattice structures," *Journal of Aerospace Engineering*, vol. 7, no. 1, pp. 72–91, 1994.

[3] F. C. Moon and G. X. Li, "Experimental study of chaotic vibrations in a pin-jointed space truss structure," *Aiaa Journal*, vol. 28, no. 5, pp. 915–921, 2012.

[4] S. P. Timoshenko and J. M. Gere, *Theory of Elastic Stability*, McGraw-Hill, New York, NY, USA, second ed. edition, 1961.

[5] A. H. Nayfeh and M. S. Hefzy, "Continuum modeling of three-dimensional truss-like space structures," *Aiaa Journal*, vol. 16, no. 8, pp. 779–787, 1978.

[6] A. H. Nayfeh and M. S. Hefzy, "Effective constitutive relations for large repetitive frame-like structures," *International Journal of Solids and Structures*, vol. 18, no. 11, pp. 975–987, 1982.

[7] U. Lee and J. Lee, "Dynamic continuum modeling of truss-type space structures using spectral elements," *Journal of Spacecraft & Rockets*, vol. 33, no. 3, pp. 404–409, 2012.

[8] A. K. Noor, W. H. Greene, and M. S. Anderson, "Continuum models for static and dynamic analyswas of repetitive lattices," in *Proceedings of the AIAA/ASME/SAE 18th Structures, Structural Dynamics and Materials Conference*, vol. 21-23, pp. 299–310, San Diego, CF, USA, March 1977.

[9] L. Usik, "Equivalent continuum models of large platelike lattice structures," *International Journal of Solids and Structures*, vol. 31, no. 4, pp. 457–467, 1994.

[10] H. Tollenaere and D. Caillerie, "Continuous modeling of lattice structures by homogenization," *Advances in Engineering Software*, vol. 29, no. 7-9, pp. 699–705, 1998.

[11] B. Burgardt and P. Cartraud, "Continuum modeling of beamlike lattice trusses using averaging methods," *Computers & Structures*, vol. 73, no. 1-5, pp. 267–279, 1999.

[12] G. Odegard, T. S. Gates, L. M. Nicholson, and K. E. Wase, "Equivalent-continuum modeling of nano-structured materials," *Composites Science and Technology*, vol. 62, no. 14, pp. 1869–1880, 2002.

[13] F. Hualin and Y. Wei, "An equivalent continuum method of lattice structures," *Acta Mechanica Solida Sinica*, vol. 19, no. 2, pp. 103–113, 2006.

[14] A. Salehian and D. J. Inman, "Micropolar continuous modeling and frequency response validation of a lattice structure," *Journal of Vibration & Acoustics*, vol. 132, no. 1, pp. 256–280, 2010.

[15] Y. W. Zhang, B. Yuan, and B. Fang, "Reducing thermal shock-induced vibration of an axially moving beam via a nonlinear energy sink," *Nonlinear Dynamics*, vol. 87, no. 2, pp. 1–9, 2017.

[16] M. H. Jalaei and Ö. Civalek, "On dynamic instability of magnetically embedded viscoelastic porous FG nanobeam," *International Journal of Engineering Science*, vol. 143, pp. 14–32, 2019.

[17] Ç. Demir and Ö. Civalek, "On the analysis of microbeams," *International Journal of Engineering Science*, vol. 121, pp. 14–33, 2017.

[18] O. Civalek, S. Dastjerdi, S. D. Akbaş, and B. Akgöz, "Vibration analysis of carbon nanotube-reinforced composite microbeams," *Mathematical Methods in the Applied Sciences*, 2020.

[19] B. Akgöz and Ö. Civalek, "Bending analysis of embedded carbon nanotubes resting on an elastic foundation using strain gradient theory," *Acta Astronautica*, vol. 119, pp. 1–12, 2016.

[20] O. V. Gendelman, "Transition of energy to a nonlinear localized mode in a highly asymmetric system of two oscillators," *Normal Modes and Localization in Nonlinear Systems*, vol. 25, no. 1, pp. 237–253, 2001.

[21] O. Gendelman, L. I. Manevitch, A. F. Vakakis, and R. M'Closkey, "Energy pumping in nonlinear mechanical oscillators: Part I-dynamics of the underlying Hamiltonian systems," *Journal of Applied Mechanics*, vol. 68, no. 1, pp. 34–41, 2001.

[22] A. F. Vakakis and O. Gendelman, "Energy pumping in nonlinear mechanical oscillators: Part II-resonance capture," *Journal of Applied Mechanics*, vol. 68, no. 1, pp. 42–48, 2001.

[23] O. Gendelman, L. I. Manevitch, and A. F. Vakakis, "A degenerate bifurcation structure in the dynamics of coupled oscillators with essential stiffness nonlinearities," *Nonlinear Dynamics*, vol. 33, no. 1, pp. 1–10, 2015.

[24] A. F. Vakakis and R. H. Rand, "Non-linear dynamics of a system of coupled oscillators with essential stiffness nonlinearities," *International Journal of Non-linear Mechanics*, vol. 39, no. 7, pp. 1079–1091, 2004.

[25] G. Kerschen, A. F. Vakakis, Y. S. Lee, D. M. Mcfarland, J. J. Kowtko, and L. A. Bergman, "Energy transfers in a system of two coupled oscillators with essential nonlinearity: 1:1 resonance manifold and transient bridging orbits," *Nonlinear Dynamics*, vol. 42, no. 3, pp. 283–303, 2005.

[26] Y. Starosvetsky and O. V. Gendelman, "Attractors of harmonically forced linear oscillator with attached nonlinear energy sink. II: optimization of a nonlinear vibration absorber," *Nonlinear Dynamics*, vol. 51, no. 1-2, p. 47, 2008.

[27] R. Viguié and G. Kerschen, "Nonlinear vibration absorber coupled to a nonlinear primary system: a tuning

methodology," *Journal of Sound and Vibration*, vol. 326, no. 3-5, pp. 780–793, 2009.

[28] C. M. Pappalardo and D. Guida, "Development of a new inertial-based vibration absorber for the active vibration control of flexible structures," *Engineering Letters*, vol. 26, no. 3, 2018.

[29] R. E. Roberson, "Synthesis of a nonlinear dynamic vibration absorber," *Journal of the Franklin Institute*, vol. 254, no. 3, pp. 205–220, 1952.

[30] S. S. Oueini, A. H. Nayfeh, and J. R. Pratt, "A nonlinear vibration absorber for flexible structures," *Nonlinear Dynamics*, vol. 15, no. 3, pp. 259–282, 1998.

[31] Y. Y. Zhao and J. Xu, "Effects of delayed feedback control on nonlinear vibration absorber system," *Journal of Sound and Vibration*, vol. 308, no. 1-2, pp. 212–230, 2007.

[32] D. M. Mcfarland, L. A. Bergman, and A. F. Vakakis, "Experimental study of non-linear energy pumping occurring at a single fast frequency," *International Journal of Non-linear Mechanics*, vol. 40, no. 6, pp. 891–899, 2005.

[33] D. M. Mcfarland, G. Kerschen, J. J. Kowtko, Y. S. Lee, L. A. Bergman, and A. F. Vakakis, "Experimental investigation of targeted energy transfers in strongly and nonlinearly coupled oscillators," *The Journal of the Acoustical Society of America*, vol. 118, no. 2, pp. 791–799, 2005.

[34] F. Georgiades and A. F. Vakakis, "Dynamics of a linear beam with an attached local nonlinear energy sink," *Communications in Nonlinear Science and Numerical Simulation*, vol. 12, no. 5, pp. 643–651, 2007.

[35] S. Tsakirtzis, A. F. Vakakis, and P. Panagopoulos, "Broadband energy exchanges between a dissipative elastic rod and a multi-degree-of-freedom dissipative essentially non-linear attachment," *International Journal of Non-linear Mechanics*, vol. 42, no. 1, pp. 36–57, 2007.

[36] P. Panagopoulos, F. Georgiades, S. Tsakirtzis, A. F. Vakakis, and L. A. Bergman, "Multi-scaled analysis of the damped dynamics of an elastic rod with an essentially nonlinear end attachment," *International Journal of Solids and Structures*, vol. 44, no. 18-19, pp. 6256–6278, 2007.

[37] A. F. Vakakis, "Passive nonlinear targeted energy transfer," *Philosophical Transactions of the Royal Society A: Mathematical, Physical and Engineering Sciences*, vol. 376, no. 2127, p. 20170132, 2018.

[38] A. F. Vakakis, O. V. Gendelman, and L. A. Bergman, *Nonlinear Targeted Energy Transfer in Mechanical and Structural Systems*, Springer, Netherlands, 2009.

[39] Y.-W. Zhang, Z. Zhang, L.-Q. Chen, T.-Z. Yang, B. Fang, and J. Zang, "Impulse-induced vibration suppression of an axially moving beam with parallel nonlinear energy sinks," *Nonlinear Dynamics*, vol. 82, no. 1-2, pp. 61–71, 2015.

[40] M. Kani, S. E. Khadem, M. H. Pashaei, and M. Dardel, "Vibration control of a nonlinear beam with a nonlinear energy sink," *Nonlinear Dynamics*, vol. 83, no. 1-2, pp. 1–22, 2015.

[41] X. Fang, J. Wen, and J. Yin, "Highly efficient continuous bistable nonlinear energy sink composed of a cantilever beam with partial constrained layer damping," *Nonlinear Dynamics*, vol. 87, no. 4, pp. 1–19, 2016.

[42] S. Bab, S. E. Khadem, and M. K. Mahdiabadi, "Vibration mitigation of a rotating beam under external periodic force using a nonlinear energy sink (NES)," *Journal of Vibration and Control*, vol. 23, no. 6, pp. 1001–1025, 2016.

[43] D. Kremer and K. Liu, "A nonlinear energy sink with an energy harvester: transient responses," *Journal of Sound and Vibration*, vol. 333, no. 20, pp. 4859–4880, 2014.

[44] D. Kremer and K. Liu, "A nonlinear energy sink with an energy harvester: harmonically forced responses," *Journal of Sound and Vibration*, vol. 410, pp. 287–302, 2017.

[45] J. E. Chen, W. He, W. Zhang, M. H. Yao, J. Liu, and M. Sun, "Vibration suppression and higher branch responses of beam with parallel nonlinear energy sinks," *Nonlinear Dynamics*, vol. 91, pp. 1–20, 2017.

[46] J. E. Chen, W. Zhang, M. H. Yao, and J. Liu, "Vibration suppression for truss core sandwich beam based on principle of nonlinear targeted energy transfer," *Composite Structures*, vol. 171, pp. 419–428, 2017.

[47] J. N. Reddy, *Mechanics of Laminated Composite Plates and Shells*, CRC Press, Boca Raton, second ed. edition, 2004.